

# Catalytic cross-coupling of diazo compounds with coinage metal-based catalysts: an experimental and theoretical study†

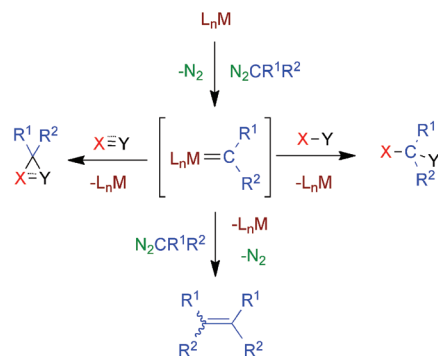
Ivan Rivilla,<sup>a</sup> W. M. C. Sameera,<sup>b</sup> Eleuterio Alvarez,<sup>c</sup> M. Mar Díaz-Requejo,<sup>\*a</sup> Feliu Maseras<sup>\*b,d</sup> and Pedro J. Pérez<sup>\*a</sup>

We examined the ability of  $\text{Tp}^x\text{M}$  ( $\text{Tp}^x$  = hydrotris(pyrazolyl)borate ligand;  $\text{M} = \text{Cu}$  and  $\text{Ag}$ ) and  $\text{IPrMCl}$  ( $\text{IPr} = 1,3\text{-bis}(\text{diisopropylphenyl})\text{imidazol-2-ylidene}$ ;  $\text{M} = \text{Cu}, \text{Ag}, \text{Au}$ ) complexes as catalyst precursors for the cross-coupling of diazo compounds. Experimental data showed that the metal centre can be tuned with the appropriate selection of the ligand to yield either the homo- or hetero-coupling (cross-coupling) products. A computational study of the reaction mechanism allowed the rationalization of the experimental reactivity patterns, and the identification of the key reaction step controlling the selectivity: the initial reaction between the metalcarbene intermediate and one of the diazo compounds.

## Introduction

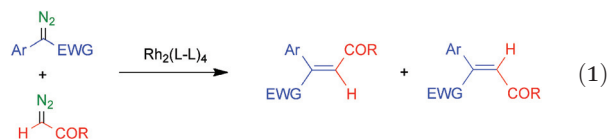
The metal-catalyzed carbene transfer reaction of diazo compounds has constituted a useful methodology in organic synthesis, both in inter- and intramolecular fashions.<sup>1</sup> During this reaction, unsaturated fragments can be modified upon addition of a  $\text{CR}^1\text{R}^2$  fragment to yield three member rings (Scheme 1). Also, saturated X–Y bonds can be functionalized, affording the corresponding insertion products.

The main drawback of all these reactions consists of the non-desired side-reaction that originates from the coupling of the metalcarbene intermediate with a second molecule of the diazo reagent (Scheme 1). Further, this homocoupling reaction is favoured over the addition/insertion processes, although the use of a low diazo concentration usually precludes such coupling. Several groups have explored this reaction as an alternative synthetic route for olefin synthesis,



**Scheme 1** Metal-catalyzed carbene transfer reactions.

where the coupling of two fragments always derives from the same diazo reagent. The ruthenium-based systems were the commonly used catalysts for this transformation,<sup>2</sup> and the transition metals from groups 4–6<sup>3</sup> and 9–11 have also been employed.<sup>4</sup> Hodgson and co-workers described<sup>5</sup> the cross-coupling of two diazoacetates of formulae  $\text{N}_2\text{C}(\text{H})\text{CO}_2\text{R}$  with different R groups. But it was not until very recently that Davies and co-workers have described a rhodium-based catalytic system to promote the efficient cross-coupling of two distinct diazo compounds<sup>6</sup> with a very high regioselectivity toward the *E* isomer [eqn (1)].



<sup>a</sup>Laboratorio de Catálisis Homogénea, Departamento de Química y Ciencias de los Materiales, Unidad Asociada al CSIC, Centro de Investigación en Química Sostenible (CIQSO), Universidad de Huelva, Campus de El Carmen s/n, 21007 Huelva, Spain. E-mail: perez@dqcm.uhu.es, mmdiaz@dqcm.uhu.es; Fax: +34-959219942

<sup>b</sup>Institute of Chemical Research of Catalonia (ICIQ), 43007 Tarragona, Catalonia, Spain. E-mail: fmaseras@icq.es; Fax: (+34) 977 920 231

<sup>c</sup>Instituto de Investigaciones Químicas, Centro de Investigaciones Isla de La Cartuja, Avda Americo Vespucio 49, 41092 Sevilla, Spain

<sup>d</sup>Departament de Química, Universitat Autònoma de Barcelona, 08193 Bellaterra, Catalonia, Spain

†Electronic supplementary information (ESI) available: Crystallographic data for compound **4** (CIF). Conformational analysis of selected structures. Evaluation of steric/electronic effects through ONIOM calculations. Total energies and Cartesian coordinates of all reported structures. CCDC 905569. For ESI and crystallographic data in CIF or other electronic format see DOI: 10.1039/c2dt32439c

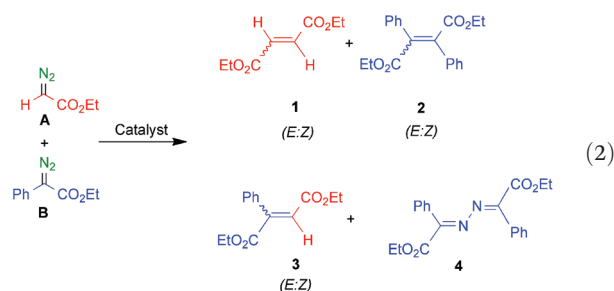
We have described several catalytic systems based on the group 11 metal complexes for the addition<sup>7</sup> or insertion<sup>8</sup> of  $\text{CHCO}_2\text{Et}$  (derived ethyl diazoacetate, EDA) to organic substrates. In view of the interest on the above cross-coupling reaction, we have studied the potential of our catalysts ( $\text{Tp}^x\text{M}$  and  $\text{IPrMCl}$ ;  $\text{Tp}^x$  = hydrotris(pyrazolyl)borate ligand;  $\text{IPr}$  = *N*-heterocyclic carbene ligand) in this transformation, where we have found that both the copper and silver can be tuned with ligands to afford the formation of desired olefins. Theoretical calculations were carried out to rationalize the mechanistic details.

## Results and discussion

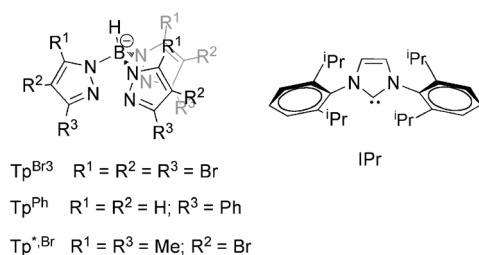
### Catalyst screening for the cross-coupling reaction of diazo compounds

Previous work carried out in our laboratory has shown that two families of group 11 metal-based catalysts containing hydrotris(pyrazolyl)borate ( $\text{Tp}^x$ ) or *N*-heterocyclic carbene (NHC) ligands (Scheme 2) readily transferred carbene units :  $\text{CHCO}_2\text{Et}$  from ethyl diazoacetate (EDA,  $\text{N}_2\text{CHCO}_2\text{Et}$ ) to several saturated or unsaturated substrates.<sup>7–9</sup> The catalytic coupling of two carbene groups was observed as a side reaction, and this process could be avoided by slow addition of EDA. The aforementioned work by Davies and co-workers<sup>6</sup> guided us to explore the catalytic potential of these compounds toward the coupling of two different diazo compounds with the aim of inducing the synthesis of the olefin derived from the cross-coupling of both carbenes.

In the first series of experiments, we tested the catalytic activity of several  $\text{Tp}^x$ -containing complexes in the cross-coupling reaction of two different diazo compounds, EDA [A in eqn (2)] and ethyl 2-phenyldiazoacetate [B in eqn (2)].



We could expect the formation of three olefins: those that are coming from the homocoupling (1, 2) and the targeted



**Scheme 2** Ligands employed in this work.

heterocoupling olefin (3) with both *Z* and *E* isomers. As shown in Table 1, the copper-based catalysts exclusively afforded a mixture of diethyl fumarate and maleate (*i.e.*, the homocoupling products from EDA). Neither of the other homocoupling olefin 2 nor the heterocoupling 3 were detected at the end of the reaction, and diazo compound B was recovered. In contrast, the analogous silver-based complexes gave 90% of the targeted cross-coupling product 3, whereas the homocoupling derivatives 1 and 2 were not formed. Different *E*:*Z* regioselectivities were induced by both silver catalysts (Table 1, entries 4, 5). Interestingly, a minor product was also formed in this case, and was identified as an azine (4) that formally derived from the coupling of two molecules of diazo compound B after the loss of a molecule of  $\text{N}_2$ . Yet described,<sup>10</sup> we have unambiguously characterized compound 4 by comparing the literature data as well as by X-ray diffraction studies (see ESI†).

After these findings, we wonder if the complexes  $\text{IPrMCl}$  ( $\text{IPr}$  = 1,3-bis(diisopropylphenyl)imidazol-2-ylidene;  $\text{M}$  = Cu, Ag and Au) could be also active for the reaction shown in eqn (2), given their already commented capabilities for carbene transfer from EDA.<sup>8a,b,11</sup> Table 2 summarizes the results that we have obtained. From which, the following information can be extracted: (i) a halide scavenger ( $\text{NaBAR}'_4$  ( $\text{Ar}'$  = 3,5-bis(trifluoromethyl) phenyl)) is required for the reaction to occur with the Cu- and Ag-based catalysts; (ii) the gold complex remained catalytically inactive with and without such a scavenger. With copper (Table 2, entry 2), homocoupling of EDA was observed as the minor product, while the cross-coupling product, 3, was obtained as the main product (89%). A similar result was observed with the silver analogue, but with the lack of 1.

**Table 1** Cross-coupling of diazo compounds A and B catalysed by  $\text{Tp}^x\text{M}$  ( $\text{M}$  = Cu, Ag)<sup>a</sup>

Entry	Catalyst	1 : 2 : 3 : 4 (%)	<i>E</i> : <i>Z</i> (3)
1 <sup>b</sup>	$\text{Tp}^{\text{Br}_3}\text{Cu}$	100 : 0 : 0 : 0	—
2 <sup>b</sup>	$\text{Tp}^{\text{Ph}}\text{Cu}$	100 : 0 : 0 : 0	—
3 <sup>b</sup>	$\text{CuI}$	100 : 0 : 0 : 0	—
4	$\text{Tp}^{*,\text{Br}}\text{Ag}$	0 : 0 : 90 : 10	78 : 22
5	$\text{Tp}^{\text{Br}_3}\text{Ag}$	0 : 0 : 90 : 10	58 : 42

<sup>a</sup> Reaction conditions: 0.0125 mmol catalyst; 5 mL  $\text{CH}_2\text{Cl}_2$ ; 0.25 mmol of each diazo compound at 5 °C. <sup>b</sup> The diazo compound B remained unreacted in the reaction mixture.

**Table 2** Cross-coupling of diazo compounds A and B using  $\text{IPrMCl}$  ( $\text{M}$  = Cu, Ag and Au) as a precatalyst<sup>a</sup>

Entry	Catalyst	1 : 2 : 3 : 4 (%)	<i>E</i> : <i>Z</i> (3)
1	$\text{IPrCuCl}$	—	—
2	$\text{IPrCuCl} + \text{NaBAR}'_4$	5 : 0 : 89 : 6	76 : 24
3	$\text{IPrAgCl}$	—	—
4	$\text{IPrAgCl} + \text{NaBAR}'_4$	0 : 0 : 91 : 9	80 : 20
5 <sup>b</sup>	$\text{IPrAuCl} + \text{NaBAR}'_4$	—	—

<sup>a</sup> Reaction conditions: 0.0125 mmol catalyst; 5 mL  $\text{CH}_2\text{Cl}_2$ ;  $\text{NaBAR}'_4$  (1 equiv.); 0.25 mmol diazo compounds at 5 °C. <sup>b</sup> Both diazo compounds remain unreacted in the reaction mixture.

Again, homocoupling of the diazo compound **B** (*i.e.*, olefin **2**) was not detected. The *E*:*Z* ratio of **3** was similar with both metals (entries 2 and 4), indicating a similar catalytic pocket. The azine, **4**, was also formed to a similar extent to that in the  $\text{Tp}^x\text{M}$  system. It is worth mentioning that the experiments were carried out upon addition of the diazo compounds in one portion at the beginning of the reaction.

The optimized results shown in Tables 1 and 2 were obtained at 5 °C, and no significant reaction outcome was observed below this temperature. When the reactions were carried out at room temperature (23 °C) with  $\text{Tp}^{\text{Br}}\text{Ag}$  and  $\text{IPrAgCl}$  as catalyst precursors, the 1:2:3:4 ratio of products found at the end of the reaction was 0:0:57:43 and 0:0:47:53, respectively. Further, both catalysts provide a significant increase of the azine, **4**. The *E*/*Z* selectivity did not change with the temperature.

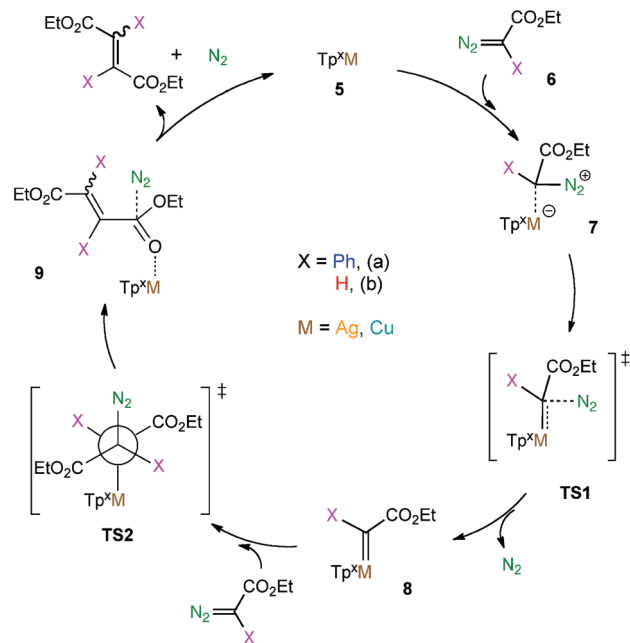
The above experimental data have shown that  $\text{Tp}^x\text{Ag}$  and  $\text{IPrMCl}$  ( $\text{M} = \text{Cu}$  and  $\text{Ag}$ ) complexes are active catalysts for the cross-coupling reaction of  $\text{N}_2\text{C}(\text{H})\text{CO}_2\text{Et}$  and  $\text{N}_2\text{C}(\text{Ph})\text{CO}_2\text{Et}$  to afford the desired heterocoupling-derived olefins **3**. Further, this is the first example of group 11 metal-based catalysts for this reaction at those levels of efficiency. A minor product was identified as the azine (**4**). On the other hand, the  $\text{Tp}^x\text{Cu}$  system exclusively led to the homocoupling products, **1**. Therefore, there is a clear effect of the ligand ( $\text{Tp}^x$  vs.  $\text{IPr}$ ) in the copper case as well as an effect of the metal,  $\text{Cu}$  vs.  $\text{Ag}$ , in the  $\text{Tp}^x$  case. In order to ascertain the nature of the mechanism that governs this transformation, a complete theoretical study has been carried out with both the  $\text{Tp}^{\text{Br}3}\text{M}$  ( $\text{M} = \text{Cu}$ ,  $\text{Ag}$ ) and  $\text{IPrMCl}$  systems ( $\text{M} = \text{Cu}$ ,  $\text{Ag}$ ,  $\text{Au}$ ), which is the subject of the next section.

## Computational studies

The proposed mechanism for the reaction of  $\text{N}_2\text{C}(\text{Ph})\text{CO}_2\text{Et}$  (**6a**) and  $\text{N}_2\text{C}(\text{H})\text{CO}_2\text{Et}$  (**6b**) catalyzed by  $\text{Tp}^x\text{M}$  (**5**) is shown in Scheme 3. The first step of this mechanism is the coordination of **6a** and **6b** to the catalyst (**5**). Starting from the resulting complexes (**7a** and **7b**),  $\text{N}_2$  dissociation leads to the active metalcarbene intermediates **8a** and **8b** via **TS1a** and **TS1b**, respectively. These metalcarbenes can react with  $\text{N}_2\text{C}(\text{Ph})\text{CO}_2\text{Et}$  (**6a**) or  $\text{N}_2\text{C}(\text{H})\text{CO}_2\text{Et}$  (**6b**) to form the cross-coupling (CC) product (**3**), homocoupling (HC) products (**1** and **2**), and azine (AZ, **4**) (see Fig. S1a, ESI†). The cross-coupling and homocoupling processes undergo through **TS2**. It is well-known from the literature<sup>12</sup> that **TS2** should have an antiperiplanar arrangement of the M–C and C–N bonds, but this leaves still some conformational flexibility associated with the approach of the two fragments. We report here only the most stable conformation of **TS2**, information on the conformational search can be found in the ESI† section.

### $\text{Tp}^{\text{Br}3}\text{M}$ systems

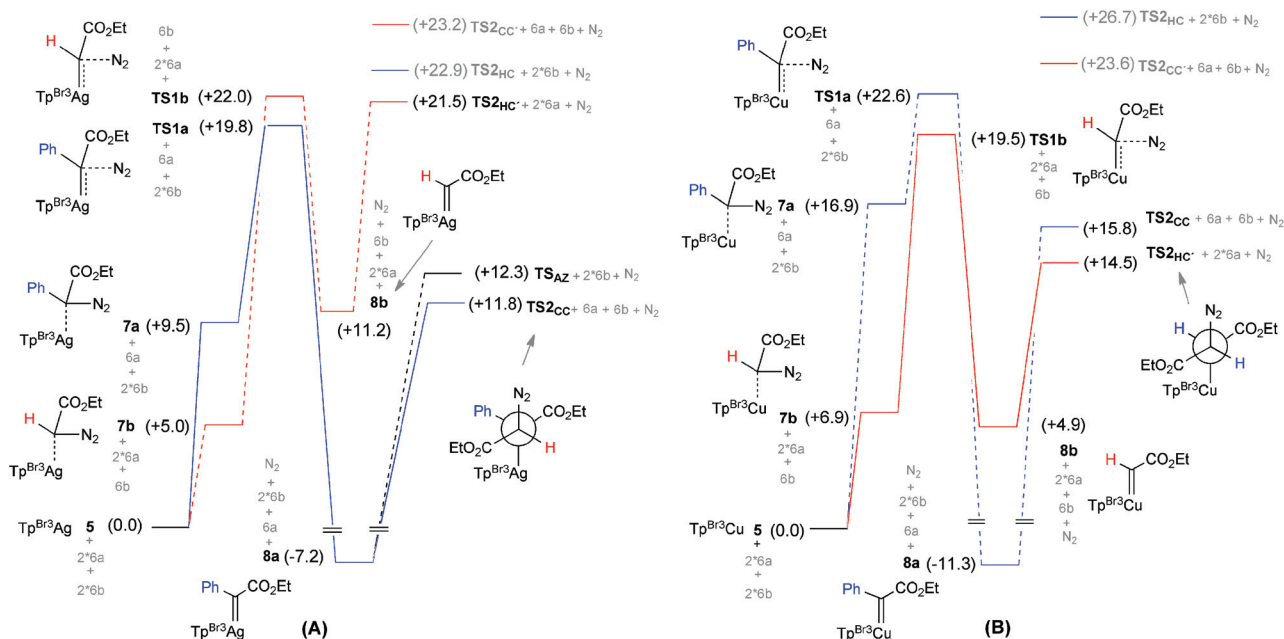
First, we computed the free energy profiles for the reaction of  $\text{N}_2\text{C}(\text{Ph})\text{CO}_2\text{Et}$  (**6a**) and  $\text{N}_2\text{C}(\text{H})\text{CO}_2\text{Et}$  (**6b**) catalyzed by



**Scheme 3** Proposed catalytic cycle for the reaction of  $\text{N}_2\text{C}(\text{Ph})\text{CO}_2\text{Et}$  (**6a**) and  $\text{N}_2\text{C}(\text{H})\text{CO}_2\text{Et}$  (**6b**) catalyzed by  $\text{Tp}^x\text{M}$  ( $\text{M} = \text{Ag}$ ,  $\text{Cu}$ ).

$\text{Tp}^{\text{Br}3}\text{Ag}$ . Results are summarized in Scheme 4A. Coordination of **6a** and **6b** on  $\text{Tp}^{\text{Br}3}\text{Ag}$  is endergonic by +9.5 (**7a**) and +5.0 (**7b**)  $\text{kcal mol}^{-1}$ , respectively. The key step happens to be the subsequent  $\text{N}_2$  elimination from **7a**, leading to the metalcarbene **8a** through transition state **TS1a** with a relative energy of 19.8  $\text{kcal mol}^{-1}$ . In a similar vein, the second metalcarbene, **8b**, can be formed through **TS1b** with a relative energy of 22.0  $\text{kcal mol}^{-1}$ . This step is critical because it constitutes the highest energy point in pathways leading to the products. The relative energies of **TS1a** and **TS1b** indicate that in the case of  $\text{Tp}^{\text{Br}3}\text{Ag}$ ,  $\text{N}_2\text{C}(\text{Ph})\text{CO}_2\text{Et}$  will react before that  $\text{N}_2\text{C}(\text{H})\text{CO}_2\text{Et}$ . We analyze the origin of the discrimination on the reaction of the first diazo molecule with the metal complex through ONIOM-(B3LYP:MM3) calculations with a mechanical embedding scheme (see Fig. S2, ESI†). This proved that the reason is *purely electronic*, when using an MM description for phenyl the discrimination disappeared.

Starting from the favoured metalcarbene (**8a**), two close energy competing pathways lead to cross-coupling product (**3**) and azine (**4**), through transition states with relative free energies of 11.8  $\text{kcal mol}^{-1}$  (**TS2<sub>CC</sub>**) and 12.3  $\text{kcal mol}^{-1}$  (**TS2<sub>AZ</sub>**), respectively. Further, these two transition states yield the 3:4 ratio of 70:30, which is in reasonable agreement with the experimental value (90:10). The most stable transition states leading to the *E* and *Z* forms of the cross-coupling products hold the barrier heights of 11.8 and 11.9  $\text{kcal mol}^{-1}$ , giving rise to the computed *E*:*Z* ratio of 54:46, which is in agreement with the experimentally observed value (58:42). In both transition states, Ag–C and C–N bonds are in the antiperiplanar conformation (Scheme 3). The favourable cross-coupling product, **3** (*E*), is –81.1  $\text{kcal mol}^{-1}$  below the entry channel



**Scheme 4** Free energy profiles (kcal mol<sup>-1</sup>) for the reaction of N<sub>2</sub>C(Ph)CO<sub>2</sub>Et (**6a**) and N<sub>2</sub>C(H)CO<sub>2</sub>Et (**6b**) catalyzed by (A) TpBr<sub>3</sub>Ag and (B) TpBr<sub>3</sub>Cu.

(not shown in the free energy profile). The alternative pathway leading to the homocoupling product (**2**) from **8a** must be discarded because of the high barrier of the transition state (22.9 kcal mol<sup>-1</sup> for TS<sub>2HC</sub>, more than 10 kcal mol<sup>-1</sup> than the competing pathways). Therefore, there is a strong preference for N<sub>2</sub>C(H)CO<sub>2</sub>Et to be the second substrate to react with the system. We attribute this preference to steric effects, as the system becomes too crowded to accept a second substrate containing a phenyl group.

For the sake of completion, we also checked the barriers for the homocoupling and cross-coupling starting from the less favourable metalcarbene, **8b**, red lines in Scheme 4A. The free energies for the corresponding transition states are prohibitively high 21.5 kcal mol<sup>-1</sup> (TS<sub>HC</sub>) and 23.2 kcal mol<sup>-1</sup> (TS<sub>CC</sub>) to compete with the pathways through **8a**. It is however worth remarking that the entry of **6a** as a second substrate molecule, leading in this case to homocoupling, is also favoured.

Calculated free energy profiles for the analogous TpBr<sub>3</sub>Cu system are shown in Scheme 4B. The most striking difference is that now the formation of **8b** has a lower free energy barrier (19.5 kcal mol<sup>-1</sup>) than that of **8a** (22.6 kcal mol<sup>-1</sup>). This is due to the fact that the coordination of N<sub>2</sub>C(Ph)CO<sub>2</sub>Et to the TpBr<sub>3</sub>Cu is difficult, as the Cu-coordination sphere (*i.e.*, Cu-ligand bond distances) is relatively smaller than the Ag-based system (Fig. 1). As a result, computed free energies of **7a** and the subsequent transition state for the N<sub>2</sub> dissociation are relatively higher in energy. Therefore, **8b** is the active metalcarbene intermediate in solution. Starting from **8b**, binding of N<sub>2</sub>C(H)CO<sub>2</sub>Et as the second diazo molecule is favored due to steric reasons, analogously to the silver system. However, in this case binding of a second unit of **6b** leads to the homocoupling product.

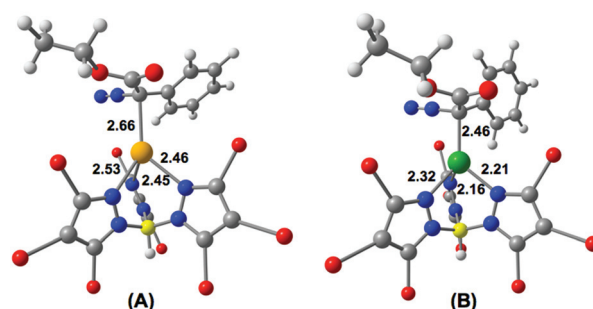


**Fig. 1** Optimised structures of **7a**: (A) Ag-based system and (B) Cu-based system.

### IPrMCl systems

According to the experimental observations, IPrCuCl and IPrAgCl systems cannot perform cross-coupling of N<sub>2</sub>C(Ph)CO<sub>2</sub>Et and N<sub>2</sub>C(H)CO<sub>2</sub>Et, and they only become active in the presence of a base, NaBAR<sub>4</sub>. This observation and previous reports in the literature<sup>11</sup> suggested that NaBAR<sub>4</sub> could abstract Cl<sup>-</sup> from IPrMCl, leading the active precursors, IPrM<sup>+</sup> that may initiate the catalytic cycle. However, the Au-based system is not active for cross-coupling or homocoupling. We carried out DFT calculations to understand these puzzling observations.

Our calculations (summarized in Scheme 5) indicated that it is more difficult to form the IPrM<sup>+</sup> active species from the starting IPrMCl + NaBPh<sub>4</sub> in the case of gold. The relative energies are 19.5 kcal mol<sup>-1</sup> for the copper system, 21.9 kcal mol<sup>-1</sup> for the silver system, and 28.0 kcal mol<sup>-1</sup> for the gold system. As a result, the availability of IPrAu<sup>+</sup> will be lower than that of IPrCu<sup>+</sup> and IPrAg<sup>+</sup>, which explains the inferior reactivity of the gold system. This is not in contradiction with the efficiency of the IPrAuCl + EDA system for other processes such as C-H

activation,<sup>11</sup> because the reactivity depends both on concentration and energy barrier.<sup>13</sup>

Our experimental results showed that both the  $\text{IPrCu}^+$  and  $\text{IPrAg}^+$  systems prefer cross-coupling rather than homocoupling. According to the free energy profiles (Scheme 6),  $\text{N}_2$  dissociation from  $\text{N}_2\text{C(Ph)CO}_2\text{Et}$  bound complex (**7a**) is easier than the  $\text{N}_2\text{C(H)CO}_2\text{Et}$  bound species (**7b**) in both systems. Therefore, the reaction passes through the metallocarbene **8a**, leading to the desired cross-coupling product, **3**. In the case of  $\text{IPrAg}^+$ , *E* and *Z* forms of **3** are formed with barriers of 15.5 and 18.2 kcal mol<sup>-1</sup>, respectively. Further, the calculated *E*:*Z* ratio of

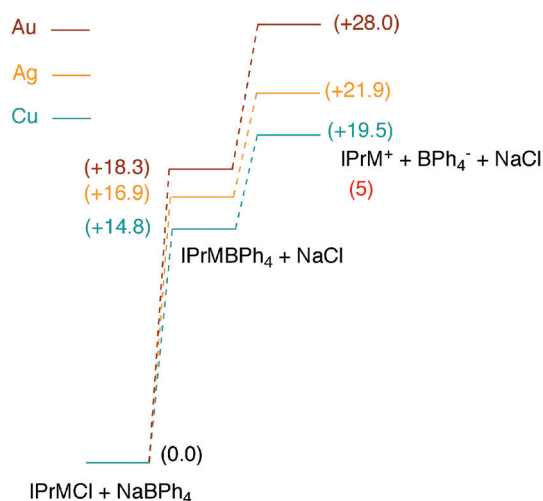
99:1 reproduced the experimental trend (*E*:*Z* = 80:20). Similar features can be seen for the analogous Cu-based system, where the calculated barriers for the *E* (17.8 kcal mol<sup>-1</sup>) and *Z* (20.4 kcal mol<sup>-1</sup>) products yield the *E*:*Z* ratio of 99:1, which also supports the experimental observations (76:24).

We observed azine as a side product with both the catalysts, and our calculated 3:4 ratio of 99:1 for the Ag-based system and 100:0 for the Cu-based system support the experimental trends. It is important to note that the  $\text{IPrCu}^+$  system provides homocoupling product (**2**) as a minor product due to the fact that the energy separation between **TS1a** and **TS1b** is only 2.6 kcal mol<sup>-1</sup>, and therefore the metallocarbene **8b** can be formed. However, we did not observe homocoupling product (**1**) in the case of  $\text{IPrAg}^+$ , because the energy gap between **TS1a** and **TS1b** is 5.5 kcal mol<sup>-1</sup>.

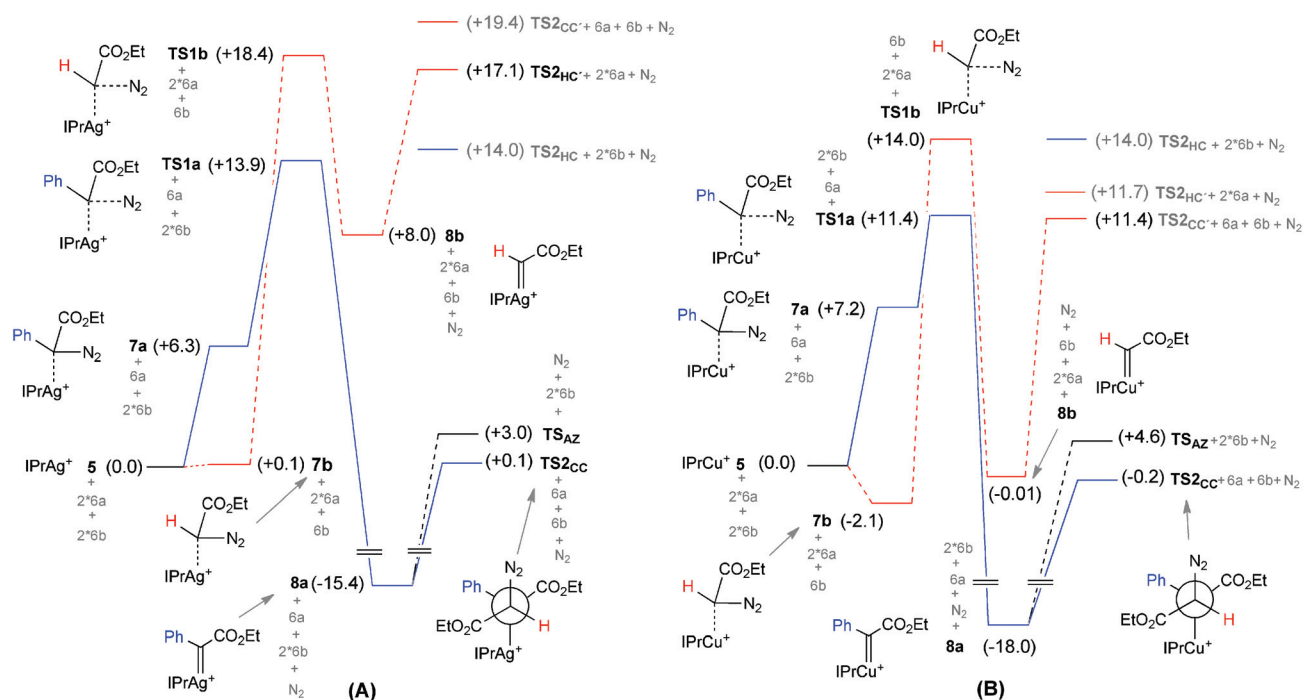
Our calculations reproduce all experimental observations, and provides a simple rationalization for them. Computational chemistry is thus a promising tool for the evaluation of the potential efficiency of new ligands for this chemical process prior to their experimental testing.

## Conclusions

We have shown that  $\text{Tp}^x\text{Ag}$  and  $\text{IPrMCl} + \text{NaBar}'_4$  (*M* = Cu and Ag) complexes are active catalysts for the cross-coupling reaction of  $\text{N}_2\text{CHCO}_2\text{Et}$  and  $\text{N}_2\text{C(Ph)CO}_2\text{Et}$  to afford heterocoupled olefins  $\text{EtO}_2\text{C(H)C=C(Ph)CO}_2\text{Et}$ , which constitute the first example of group 11 metal-based catalysts at this level of efficiency. The related  $\text{Tp}^x\text{Cu}$  complexes exclusively lead to the



**Scheme 5** Free energy profiles (kcal mol<sup>-1</sup>) for the formation of  $\text{IPrM}^+$  from  $\text{IPrMCl}$ .



**Scheme 6** Free energy profiles (kcal mol<sup>-1</sup>) for the reaction of  $\text{N}_2\text{C(Ph)CO}_2\text{Et}$  and  $\text{N}_2\text{C(H)CO}_2\text{Et}$  catalyzed by (A)  $\text{IPrAg}^+$  and (B)  $\text{IPrCu}^+$ .



homocoupling products,  $\text{EtO}_2\text{C}(\text{H})\text{C}=\text{C}(\text{H})\text{CO}_2\text{Et}$ .  $\text{IPrAuCl}$  does not react under similar conditions.

This diverse reactivity could be explained by a computational study on the reaction mechanism. The reaction takes place in a mononuclear complex, with one diazo compound reacting sequentially after the other. In all reacting systems except  $\text{Tp}^*\text{Cu}$ , the initial reaction with  $\text{N}_2\text{C}(\text{Ph})\text{CO}_2\text{Et}$  is favored because of electronic reasons.

The second diazo compound to react is always  $\text{N}_2\text{C}(\text{H})\text{CO}_2\text{Et}$  due to steric reasons. As a result, the heterocoupling product is obtained from  $\text{Tp}^*\text{Ag}$  and  $\text{IPrMCl}$  ( $\text{M} = \text{Cu}$  and  $\text{Ag}$ ), and the homocoupling product from  $\text{Tp}^*\text{Cu}$ . The lack of reactivity of  $\text{IPrAuCl}$  is satisfactorily explained by the higher energy cost of displacement of the  $\text{Cl}^-$  group to produce the active catalyst.

## Experimental section

### General manipulations

All experiments were performed using conventional vacuum line and Schlenk techniques or in a drybox. The complexes  $\text{Tp}^*\text{M}^{14}$  and  $\text{IPrMCl}^{15}$  were prepared according to literature procedures as well as the diazo compounds ethyl-2-diazoacetate-2-phenylacetate<sup>16</sup> and  $\text{NaBAR}'_4$  ( $\text{Ar}' = \text{tetrakis}(3,5\text{-bis}(\text{trifluoromethyl})\text{phenyl})\text{borate}$ ).<sup>17</sup> Ethyl diazoacetate was purchased from Sigma Aldrich. NMR spectra were recorded at 298 K using a Varian Mercury 400 instrument. GC were run in a Varian 3900 model.

### General catalytic reaction

In a typical experiment, the catalyst (0.0125 mmol) was dissolved in 5 mL of the  $\text{CH}_2\text{Cl}_2$ . In the case of  $\text{IPrMCl}$  complexes, 1 equiv. of  $\text{NaBAR}'_4$  was added to the above solution. Then, ethyl-2-diazoacetate (0.25 mmol) and ethyl-2-diazoacetate-2-phenylacetate (0.25 mmol) were added in one portion. The reaction mixture was stirred at 5 °C until no diazo reagents were detected by GC. The volatiles were removed under vacuum, and the residue was purified by  $\text{SiO}_2$ -column chromatography with  $\text{AcOEt}$ -petroleum ether (10:1). NMR studies revealed the formation of three products (see eqn (2)). The compounds were identified by comparing with the literature data.<sup>10,18</sup>

### Computational details

All calculations were performed using DFT with the B3LYP functional as implemented in the Gaussian09 program.<sup>19</sup> The LanL2DZ<sup>20</sup> basis set and associated effective core potentials with a single  $f$  polarization function were used for Ag (1.611), Cu (3.525), and a  $d$  polarization was added for Br (0.4280).<sup>21</sup> The 6-31G(d) basis set was used for the C, H, N, O, and B atoms.<sup>22</sup> The SMD approach of Truhlar and co-workers was applied for solvation treatments,<sup>23</sup> where dichloromethane ( $\epsilon = 8.93$ ) was used as the solvent. All structure optimizations were full in the solvent phase with no restrictions, and vibrational frequency calculations were performed in order to confirm

that the stationary points were minima or transition states. All transition states had a single imaginary frequency in the optimization in solvent phase. Free energy corrections at 298.15 K and  $10^5$  Pa pressure were used, including zero point energy corrections. Connectivity of the transition state structures was confirmed by relaxing the transition state geometry towards both the reactant and the product. Single-point test calculations with M06 and B97D produced slightly worse agreement with experiment than the B3LYP calculations, there seems to be some problem with the introduction of dispersion corrections in these systems.

Hybrid quantum mechanics/molecular mechanics (QM:MM)<sup>24</sup> calculations were performed with a new ONIOM-(DFT:MM3) implementation developed by our group, where we used the Gaussian09 standardized interface to run Tinker6.0.<sup>25</sup>

## Acknowledgements

We thank MINECO (CTQ2011-28942-CO2-01, CTQ2011-27033 and Consolider Ingenio 2010 CSD2006-0003), Junta de Andalucía (Proyecto P10-FQM-06292), Generalitat de Catalunya (2009SGR-2059 and Xarxa de Referència en Química Teòrica i Computacional) and the ICIQ Foundation for financial support.

## Notes and references

- (a) M. P. Doyle, R. Duffy, M. Ratnikov and L. Zhou, *Chem. Rev.*, 2010, **110**, 704–724; (b) M. P. Doyle, M. A. McKervey and T. Ye, *Modern Catalytic Methods for Organic Synthesis with Diazo Compounds*, John Wiley & Sons, New York, 1998; (c) G. Maas, *Top. Curr. Chem.*, 1987, **137**, 75–253.
- Ruthenium-based catalysts: (a) L. K. Woo and D. A. Smith, *Organometallics*, 1992, **11**, 2344–2346; (b) J. P. Collman, E. Rose and G. D. Venburg, *J. Chem. Soc., Chem. Commun.*, 1993, 934–935; (c) W. Baratta, A. D. Zotto and P. Rigo, *Chem. Commun.*, 1997, 2163–2164; (d) W. Baratta, A. D. Zotto and P. Rigo, *Organometallics*, 1999, **18**, 5091–5096; (e) E. Graban and F. R. Lemke, *Organometallics*, 2002, **21**, 3823–3826; (f) G.-Y. Li and C.-M. Che, *Org. Lett.*, 2004, **6**, 1621–1623.
- Groups 4–6 metal-based catalysts: (a) J. Goux, P. L. Gendre, P. Richard and C. Moïse, *J. Organomet. Chem.*, 2006, **691**, 3239–3244; (b) J. Pfeiffer and K. H. Dötz, *Angew. Chem., Int. Ed. Engl.*, 1997, **36**, 2828–2830; (c) D. Jan, F. Simal, A. Demonceau, A. F. Noels, K. A. Rufanov, N. A. Ustynyuk and D. N. Gourevitch, *Tetrahedron Lett.*, 1999, **40**, 5695–5699; (d) Z. Zhu and J. H. Espenson, *J. Am. Chem. Soc.*, 1996, **118**, 9901–9907.
- Groups 9–11 metal-based catalysts: (a) T. Kubo, S. Sakaguchi and Y. Ishii, *Chem. Commun.*, 2000, 625–626; (b) H. Bock and H. P. Wolf, *J. Chem. Soc., Chem. Commun.*,

- 1990, 690–692; (c) T. Oshima and T. Nagai, *Tetrahedron Lett.*, 1980, **21**, 1251–1254.
- 5 D. M. Hodgson and D. Angrish, *Chem.–Eur. J.*, 2007, **13**, 3470–3479.
- 6 J. H. Hansen, B. T. Parr, P. Pelphrey, Q. Jin, J. Autschbach and H. M. L. Davies, *Angew. Chem., Int. Ed.*, 2011, **50**, 1–6.
- 7 Addition reactions. Cyclopropanation: (a) M. M. Díaz-Requejo, A. Caballero, T. R. Belderrain, M. C. Nicasio, S. Trofimenko and P. J. Pérez, *J. Am. Chem. Soc.*, 2002, **124**, 978–983; Cyclopropenation: (b) M. M. Díaz-Requejo, M. A. Mairena, T. R. Belderrain, M. C. Nicasio, S. Trofimenko and P. J. Pérez, *Chem. Commun.*, 2001, 1804–1805.
- 8 Insertion reactions. C–H bonds: (a) M. M. Díaz-Requejo and P. J. Pérez, *Chem. Rev.*, 2008, **108**, 3379–3394; (b) M. M. Díaz-Requejo, T. R. Belderrain, M. C. Nicasio and P. J. Pérez, *Dalton Trans.*, 2006, 5559–5566. N–H bonds: (c) M. E. Morilla, M. M. Díaz-Requejo, T. R. Belderrain, M. C. Nicasio, S. Trofimenko and P. J. Pérez, *Chem. Commun.*, 2002, 2998–2999; O–H bonds: (d) M. E. Morilla, M. M. Díaz-Requejo, T. R. Belderrain, M. C. Nicasio, S. Trofimenko and P. J. Pérez, *Organometallics*, 2003, **22**, 2914–2918.
- 9 For reviews see: (a) M. M. Díaz-Requejo and P. J. Pérez, *J. Organomet. Chem.*, 2005, **690**, 5441–5450; (b) M. M. Díaz-Requejo and P. J. Pérez, *J. Organomet. Chem.*, 2001, **617**, 110–118.
- 10 R. Glaser, G. S. Chen and C. L. Barnes, *J. Org. Chem.*, 1993, **58**, 7446–7455.
- 11 (a) M. R. Fructos, T. R. Belderrain, P. de Frémont, N. M. Scott, S. P. Nolan, M. M. Díaz-Requejo and P. J. Pérez, *Angew. Chem., Int. Ed.*, 2005, **44**, 5284–5288; (b) M. R. Fructos, P. de Frémont, S. P. Nolan, M. M. Díaz-Requejo and P. J. Pérez, *Organometallics*, 2006, **25**, 2237–2241.
- 12 (a) D. S. Wulfman, B. W. Peace and R. S. McDaniel Jr., *Tetrahedron*, 1976, **32**, 1251–2155; (b) T. Oshima and T. Nagai, *Tetrahedron Lett.*, 1980, **21**, 1251–2154; (c) B. K. R. Shankar and H. Shechter, *Tetrahedron Lett.*, 1982, **23**, 2277–2280; (d) J. Hansen, J. Autschbach and H. M. L. Davies, *J. Org. Chem.*, 2009, **74**, 6555–6563; (e) J. H. Hansen, B. T. Parr, P. Pelphrey, Q. Jin, J. Autschbach and H. M. L. Davies, *Angew. Chem., Int. Ed.*, 2011, **50**, 2544–2548.
- 13 A. A. C. Braga, E. Álvarez, A. Caballero, J. Urbano, M. M. Díaz-Requejo, P. J. Pérez and F. Maseras, *ChemCatChem*, 2011, **3**, 1646–1652.
- 14 (a) C. Mealli, C. S. Arcus, J. L. Wilkinson, T. J. Marks and J. Ibers, *J. Am. Chem. Soc.*, 1976, **98**, 711–718; (b) J. L. Schneider, S. M. Carrier, C. E. Ruggiero, V. G. Young Jr. and W. B. Tolman, *J. Am. Chem. Soc.*, 1998, **120**, 11408–11418; (c) M. A. Mairena, J. Urbano, J. Carbajo, J. J. Maraver, E. Alvarez, M. M. Díaz-Requejo and P. J. Pérez, *Inorg. Chem.*, 2007, **46**, 7428–7435.
- 15 (a) V. Jurkauskas, J. P. Sadighi and S. L. Buchwald, *Org. Lett.*, 2003, **5**, 2417–2420; (b) H. Kaur, F. K. Zinn, E. D. Stevens and S. P. Nolan, *Organometallics*, 2004, **23**, 1157–1160; (c) L. Dang, Z. Lin and T. B. Marder, *Organometallics*, 2010, **29**, 917–927; (d) M. Delgado-Rebollo, Á. Beltrán, A. Prieto, M. M. Díaz-Requejo, A. M. Echavarren and P. J. Pérez, *Eur. J. Inorg. Chem.*, 2012, **9**, 1380–1386.
- 16 S. Bachmann, D. Fielenbach and K. A. Jørgensen, *Org. Biomol. Chem.*, 2004, **2**, 3044–3049.
- 17 (a) M. Brookhart, B. Grant and A. F. Volpe, *Organometallics*, 1992, **11**, 3920–3922; (b) H. Iwamoto, T. Sonoda and H. Kobayashi, *Tetrahedron Lett.*, 1983, **24**, 4703–4706.
- 18 (a) D. Avoiac, L. Rombinaic, H. Mani-Ronchin and G. Verardo, *J. Chem. Soc., Chem. Commun.*, 1981, 541–542; (b) L. Zhou, W. Zhang and H. F. Jiang, *Sci. China, Ser B: Chem.*, 2008, **51**, 241–247.
- 19 M. J. Frisch, G. W. Trucks, H. B. Schlegel, G. E. Scuseria, M. A. Robb, J. R. Cheeseman, G. Scalmani, V. Barone, B. Mennucci, G. A. Petersson, H. Nakatsuji, M. Caricato, X. Li, H. P. Hratchian, A. F. Izmaylov, J. Bloino, G. Zheng, J. L. Sonnenberg, M. Hada, M. Ehara, K. Toyota, R. Fukuda, J. Hasegawa, M. Ishida, T. Nakajima, Y. Honda, O. Kitao, H. Nakai, T. Vreven, J. A. Montgomery Jr., J. E. Peralta, F. Ogliaro, M. Bearpark, J. J. Heyd, E. Brothers, K. N. Kudin, V. N. Staroverov, R. Kobayashi, J. Normand, K. Raghavachari, A. Rendell, J. C. Burant, S. S. Iyengar, J. Tomasi, M. Cossi, N. Rega, J. M. Millam, M. Klene, J. E. Knox, J. B. Cross, V. Bakken, C. Adamo, J. Jaramillo, R. Gomperts, R. E. Stratmann, O. Yazyev, A. J. Austin, R. Cammi, C. Pomelli, J. W. Ochterski, R. L. Martin, K. Morokuma, V. G. Zakrzewski, G. A. Voth, P. Salvador, J. J. Dannenberg, S. Dapprich, A. D. Daniels, Ö. Farkas, J. B. Foresman, J. V. Ortiz, J. Cioslowski and D. J. Fox, *GAUSSIAN 09 (Revision A.1)*, Gaussian, Inc., Wallingford CT, 2009.
- 20 (a) P. J. Hay and W. R. Wadt, *J. Chem. Phys.*, 1985, **82**, 270–283; (b) W. R. Wadt and P. J. Hay, *J. Chem. Phys.*, 1985, **82**, 284–298; (c) P. J. Hay and W. R. Wadt, *J. Chem. Phys.*, 1985, **82**, 299–310.
- 21 (a) A. Höllwarth, M. Böhme, S. Dapprich, A. W. Ehlers, A. Gobbi, V. Jonas, K. F. Köhler, R. Stegmann, A. Veldkamp and G. Frenking, *Chem. Phys. Lett.*, 1993, **208**, 237–240.
- 22 (a) W. J. Hehre, R. Ditchfield and J. A. Pople, *J. Chem. Phys.*, 1972, **56**, 2257–2261; (b) P. C. Hariharan and J. A. Pople, *Theor. Chim. Acta*, 1973, **28**, 213–222; (c) M. S. Gordon, *Chem. Phys.*, 1980, **76**, 163–168.
- 23 A. V. Marenich, C. J. Cramer and D. G. Truhlar, *J. Phys. Chem. B*, 2009, **113**, 6378–6396.
- 24 (a) G. Ujaque and F. Maseras, *Struct. Bonding*, 2004, **112**, 117–149; (b) T. Vreven, K. S. Byun, I. Komaromi, S. Dapprich, J. A. Montgomery, K. Morokuma and M. J. Frisch, *J. Chem. Theory Comput.*, 2006, **2**, 815–826; (c) C. Bo and F. Maseras, *Dalton Trans.*, 2008, 2911–2919; (d) W. M. C. Sameera and F. Maseras, *WIREs Comput. Mol. Sci.*, 2012, **2**, 375–385.
- 25 (a) P. Ren and J. W. Ponder, *J. Phys. Chem. B*, 2003, **107**, 5933–5947; (b) M. J. Schnieders and J. W. Ponder, *J. Chem. Theory Comput.*, 2007, **3**, 2083–2097; (c) P. Ren, C. Wu and J. W. Ponder, *J. Chem. Theory Comput.*, 2011, **7**, 3143–3161.